materials proceedings

MDPI

Proceeding Paper

Camellia sinensis and *Cocos nucifera* Derived Gold Nanoparticles for Treatment of Infections Caused by Antibiotic Resistant *Staphylococcus aureus* †

Saman Anwar, Sidra Altaf, Muhammad Saif Ur Rehman Babar, M. Bilal Aslam, Humaira Muzaffar and Arsalan Iftikhar

† Presented at the 4th International Online Conference on Nanomaterials, 5–19 May 2023; Available online: https://iocn2023.sciforum.net.

Highlights:

- Development of gold nanoparticles by using green nanotechnology.
- Characterization of gold nanoparticles via UV-Visible spectroscopy, X-ray diffraction (XRD), Scanning electron microscope (SEM), Transmission electron microscopy (TEM), Dynamic Light Scattering (DLS) and Fourier Transform Infrared Spectroscopy (FTIR).
- Evaluate the therapeutic potential of green gold nanoparticles against antibiotic resistant *Staphylococcus aureus.*

Abstract: Development of bacterial resistance towards existing antibiotics is a universal problem for human and animal health as well as for food security. In an attempt to overcome this problem, nanotechnology has contributed with nano formulations. However, these are associated with risks and drawbacks including environmental toxicity, cell injury, issues of high production cost and scarcity of active ingredients. On the other hand, green synthesis of nano formulations by biological methods is a simple, innovative, ecofriendly, cost effective and advanced approach for the treatment of lethal infections caused by multidrug resistant organisms like staphylococcus aureus. *About 30% of humans are asymptomatic carriers of S. aureus in their upper respiratory tract*. Clinical disease caused by *S. aureus* infections range from mild to severe and may be manifested in the form of pneumonia, osteomyelitis, skin and deep tissue infections Here, we prepared plant-mediated gold nanoparticles from *Camellia sinensis* and *Cocos nucifera*. The green biocompatible nanoparticles were characterized by using UV-Visible spectroscopy (UV-Vis. spectroscopy), X-ray diffraction (XRD), Scanning electron microscope (SEM), Transmission electron microscopy (TEM), Dynamic light scattering (DLS) and Fourier transform infrared spectroscopy (FTIR). Moreover, these green gold nanoparticles were investigated for their antimicrobial activity by checking minimum inhibitory concentration (MIC). We found that the newly developed bio-nanoparticles showed strong activity against the multidrug resistant *Staphylococcus aureus.*

Keywords: gold nanoparticles; green nanotechnology; *Camellia sinensis; Cocos nucifera;* antibiotic resistant; ampicillin

1. Introduction

Staphylococcus aureus is a gram positive bacterium that occurs as a common member of microbiota of the body and is usually present in clinical sites across the world [1]. About 30% of humans are asymptomatic carriers of *S. aureus* in their upper respiratory tract [2]. Additionally, around 80% of invasive *S. aureus* infections arise from a strain of hosts microflora [3]. Clinical disease caused by *S. aureus* infections range from mild to severe and may be manifested in the form of pneumonia, osteomyelitis, skin and deep tissue infections. Treatment of *S. aureus* infections is becoming increasingly difficult due to antibiotic

resistance. Antibiotic resistance does not only harm the humans health but also affects the economy of the developing and the developed countries [4]. Every year 95,000 invasive multidrug-resistant *S. aureus* infections occur in the United States only [2]. According to WHO assessments, infections of multidrug-resistant *S. aureus* account for more than 25,000 deaths each year, which will grow to a whopping 10 million count in 2050 [4]. Extremely virulent antibiotic-resistant strain of *S. aureus* is ampicillin-resistant strain [5]. Several pharmaceutical formulations like penicillins, sulfonamides, tetracyclines and glycopeptides are available for the treatment of *S. aureus* infections. These antibiotics show several side effects and are expensive especially in developing countries like Pakistan, India and Bangladesh. Most importantly resistance is developing against these potent antibiotics. To overcome these effects, bionanoformulation has been designed.

Nanotechnology is a developing division of pharmaceutical science wherein the particles restrict to nanosize [6,7]. Nanoparticles prepared by various physical and chemical methods are not highly recommended due to their toxic effects however, those prepared by biological methods are preferred due to beneficial features including cost-effectiveness, biocompatibility, biodegradability and eco-friendliness and green synthesis affords good source for high productivity and purity because toxic chemicals and hazardous substances are avoided in the manufacturing process of nanoparticles [8].

Metallic nanoparticles are used for different pharmaceuticals, agricultural and medicinal applications [9]. Their essential features like physicochemical properties, electronic and optics properties can be fine-turned by altering the characterization of nanoparticles for example aspect format, size and shape [10]. Numerous metals and their oxides are being used in biological systems as nanoparticles because of their easy production and promising optical properties [11]. Moreover, the metals derived from plants have extreme potential to improve human health if applied in the agricultural, food and biomedical fields [12].

Green synthesis is the amalgamation of nanoparticles with plants and their metabolites. In the green nanotechnology, biological substances are utilized to formulate the nanoparticles for the pharmaceutical and other applications. Synthesis of nanoparticles by green biological methods are highly beneficial because of having the ability to curtail toxic effects of nanoparticles [6]. Gold nanoparticles synthesized by green nanotechnology are biocompatible and biodegradable as these nanoparticles are obtained from natural plant sources and no toxic chemical agent is consumed during preparation [13]. Green nanoparticles are economical as compared to conventional brands of drugs.

Antibacterial agents are basically significant in decreasing the load of infectious disorders. Development and spreading of multi-drug resistant strains of pathogenic bacteria is a significant and lethal public health hazard as there are few or even sometimes, no effective antibacterial agents accessible for the infection produced by resistant pathogenic bacteria [14]. There is an ultimate need to develop a potent therapeutic agent for the treatment of such lethal pathogenic infections. We have prepared and characterized gold nanoparticles from CSE and CNW and investigated the newly developed nanodrug against the deadly S. aureus infection.

2. Materials and Methods

Preparation of Camellia sinensis extracts (CSE):

One (g) of *Camellia sinensis* leaves was added in 50 mL boiling water, filtered the extract and stirred them with the help of magnetic stirrer for 30 min [10].

Preparation of Tetra chloro auric acid solution:

A 3.9 mg tetra chloro auric acid was weighing and mixes it with 100µL of deionized water.

Preparation of gold nanoparticles via CS plant:

Camellia sinensis extract (9.9 mL) in a beaker and add 3.9 mg tetra chloro auric acid in 100µL of deionized water. This solution was stirred with the help of magnetic stirrer for 15 min. Color of this solution initially changed from pale yellow to purple red color and

it indicated the formation of gold nanoparticles. Additionally, this solution was mixed for 20 min.

Preparation of gold nanoparticles via CN plant:

Cocos nucifera water (9.9 mL) in a beaker and add 3.9 mg tetra chloro auric acid in 100µL of deionized water. This solution was stirred with the help of magnetic stirrer for 30 min. Color of this solution initially changed from pale yellow to purple red color and it indicated the formation of gold nanoparticles. Additionally, this solution was mixed for 20 min. Preparation of green gold nanoparticles from *Camellia sinensis* and *Cocos nucifera* are summarized in Figure 1.

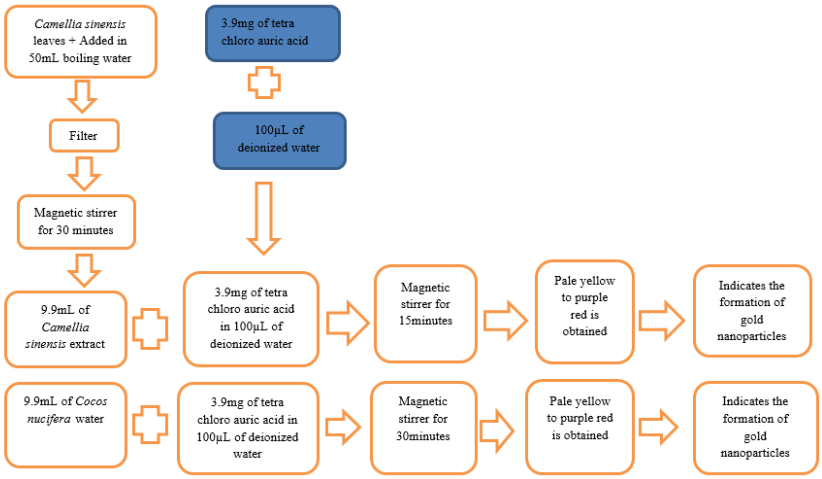

Figure 1. Summary of preparation of gold nanoparticles from *Camellia sinensis* and *Cocos nucifera.*

Dynamic light scattering

Dynamic light scattering (DLS) was used to define the size dispersal profile of gold NPs.

UV-Visible spectroscopy

UV-Visible spectroscopy (UV-Vis spectroscopy) was used to determine the absorbance of gold nanoparticles.

Fourier Transform Infrared Spectroscopy

Fourier Transform Infrared Spectroscopy (FTIR) was used to provide information of the chemical composition and physical state of the gold NPs.

Scanning electron microscope

Scanning electron microscope (*SEM)* was used to produce images of a sample by scanning the surface with a focused beam of electrons.

Transmission electron microscopy

Transmission electron microscopy (TEM) (200 kV) was used to check the image of gold NPs.

Energy dispersive X-ray spectroscopy

Energy dispersive X-ray spectroscopy (XRD) was used to determine the crystallographic structure of nanoparticles.

Antimicrobial activity

The zone of inhibition was calculated using the well diffusion method on an agar plate. Pathogenic bacteria *Staphylococcus aureus* was grown overnight at 4 °C on Mueller Hinton agar plates. Each bacterium was grown its own sterile Mueller Hinton agar plate in this process. Using sterile cotton swabs, pathogenic bacteria were coated on the agar plate and these plates was dried. A sterile well cutter (6 mm in diameter) can drill wells in each agar plate. The nanoparticle suspension was poured into wells. For full diffusion, these plates was placed for 1 h and then incubated at 37 °C for 1 day and the diameter of inhibitory zones will be measured in mm [15].

Minimum inhibitory concentration (MIC)

Standard inoculum (10^5 CFU/mL) for determination of MIC was prepared by Broth Micro Dilution method. Microtitration plate of 96 wells was filled with nutrient broth. Leaving one positive control and one negative control, serial two-fold dilutions of gold nanoparticles in concentrations ranging from 3.9 mg/µL, 10 mg/µL, 30 mg/µL and 50 mg/µL with adjusted bacterial concentration used to determine MIC. This experiment incorporated a positive control having a nutrient broth media, inoculum and a negative control having a nutrient broth media. Plate was incubated at 37° C and check for 24 h. Optical density (OD) values before and after incubation was measured at 625 nm wavelength, using spectrophotometer. Net OD value was determined and compared with cutoff value to find minimum inhibitory concentration of these preparations of gold nanoparticles [16].

3. Results

Characterization of gold nanoparticles

Physical appearance:

Preparation of gold nanoparticles was commonly confirmed by color identifications. Through the experimentation, the appearance of purple red color suspension from the initial pale yellow color shows the formation of gold nanoparticle that is mediated by CSE and the appearance of purple red color suspension from the CNW shows the formation of gold nanoparticle that is mediated by CN plant. Preparation of CSNp and CNNp were shown in Figures 2 and 3.

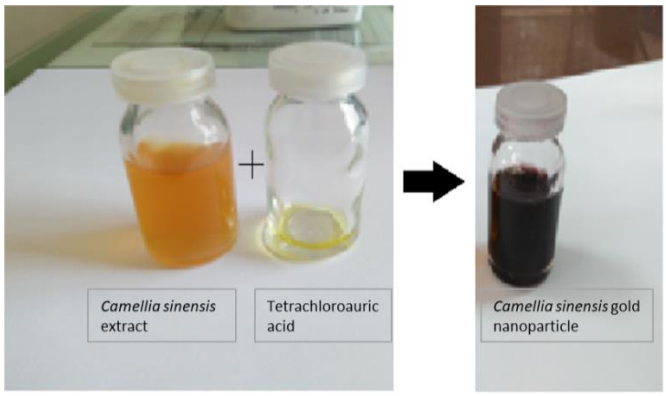

Figure 2. Gold nanoparticles prepared by *Camellia sinensis* plant.

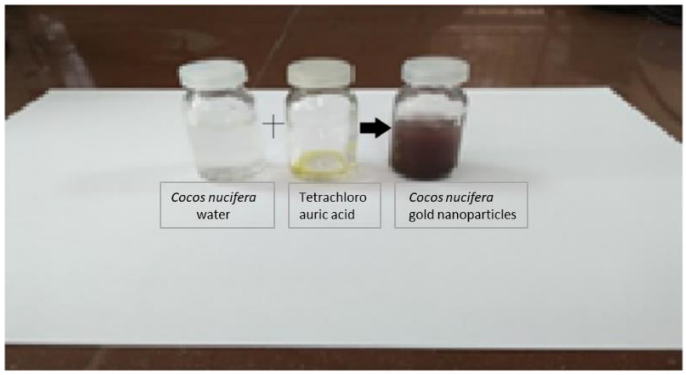

Figure 3. Gold nanoparticles prepared by *Cocos nucifera* plant.

Zeta size and Zeta potential:

Zeta size gives an estimate of mean particles size and their poly dispersity index (PDI). Average zeta size of CSNp is 41.61 nm and CNNp is 34.12 nm. Zeta size of the nanoparticles is given in the (Table 1) along with zeta scan results in Figure 4a,b. Zeta potential of CSNp is −16.52 mv and CNNp is −14.61 mv. Zeta potential of the nanoparticles is given in the (Table 1) along with zeta scan results in Figure 5a,b.

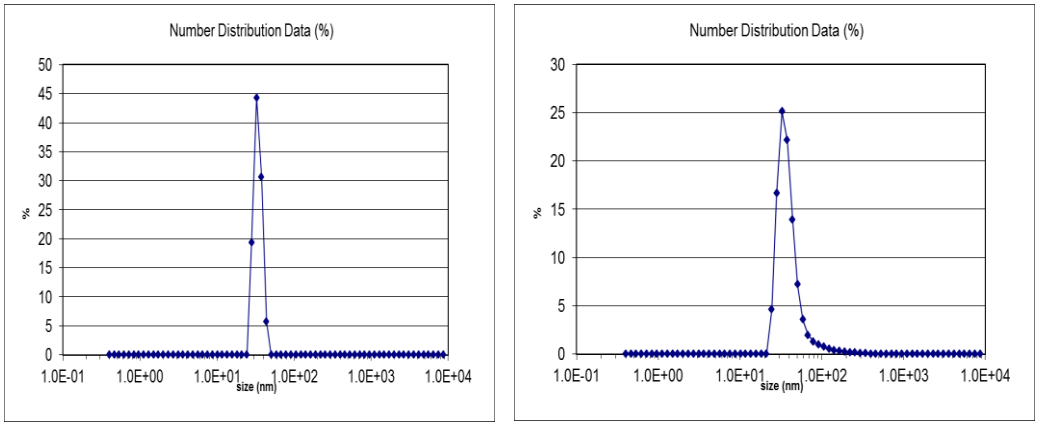

(**a**) (**b**)

Figure 4. (**a**) Zeta size of CSNp; (**b**) Zeta size of CNNp.

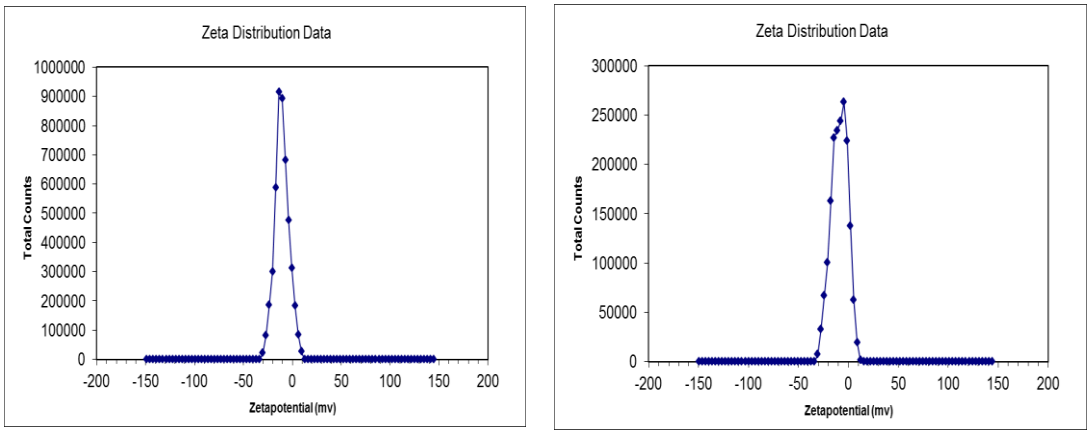

(**a**) (**b**)

Figure 5. (**a**) Zeta potential of CNNp; (**b**) Zeta potential of CSNp.

Table 1. Zeta size and zeta potential of CSNp and CNNp.

Formulations	Z-Average (nm)	PDI	Zeta Potential
CSNp	41.61	0.245	−16.52
CNNp	34.12	1	−14.61

Fourier Transform Infrared Spectroscopy

CSE and CSNp both have same peaks that mean gold nanoparticles prepared by extract was confirmed. CNW and CNNp both have same peaks that mean gold nanoparticles prepared by coconut water was confirmed. These graphs were shown in Figure 6a,b.

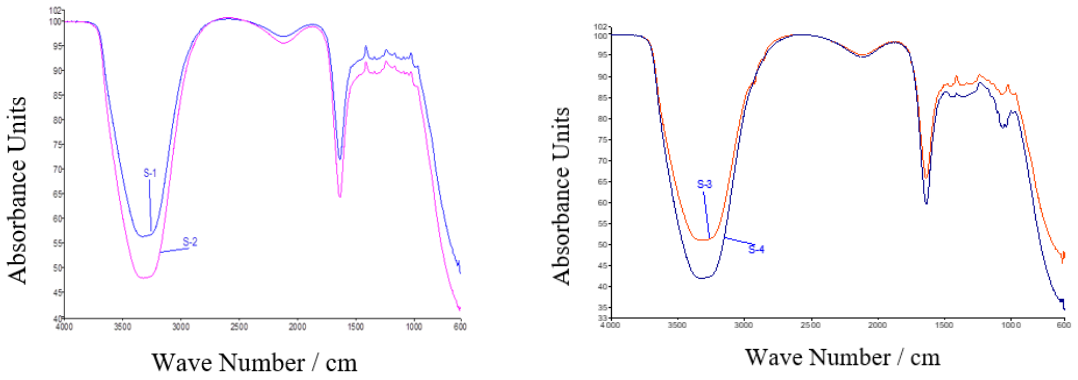

(**a**) (**b**)

Figure 6. Whereas, S1: CSE; S2: CSNp; S3: CNW; S4: CNNp.

Scanning electron microscopy

Scanning electron microscope (SEM) presented the image of gold nanoparticles. SEM represents the morphology of the gold nanoparticles that is prepared from CSE and CNW have spherical shape. SEM images were shown in Figure 7a,b.

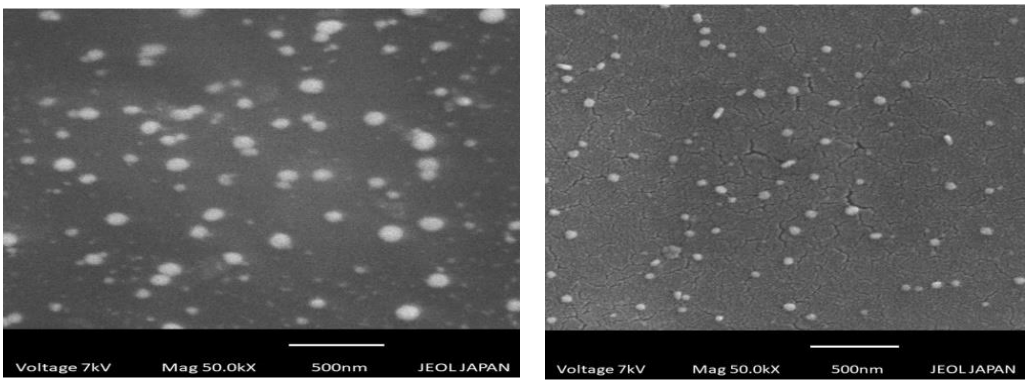

(**a**) (**b**)

Figure 7. (**a**) SEM images of CNNp; (**b**) SEM images of CSNp.

Transmission electron microscopy

Transmission electron microscopy (TEM) is used to present the image of gold nanoparticles. TEM represents a highly-magnified image that is prepared from CSE and CNW. TEM is also magnifying images up to 2 million times. TEM images were shown in Figure 8a,b.

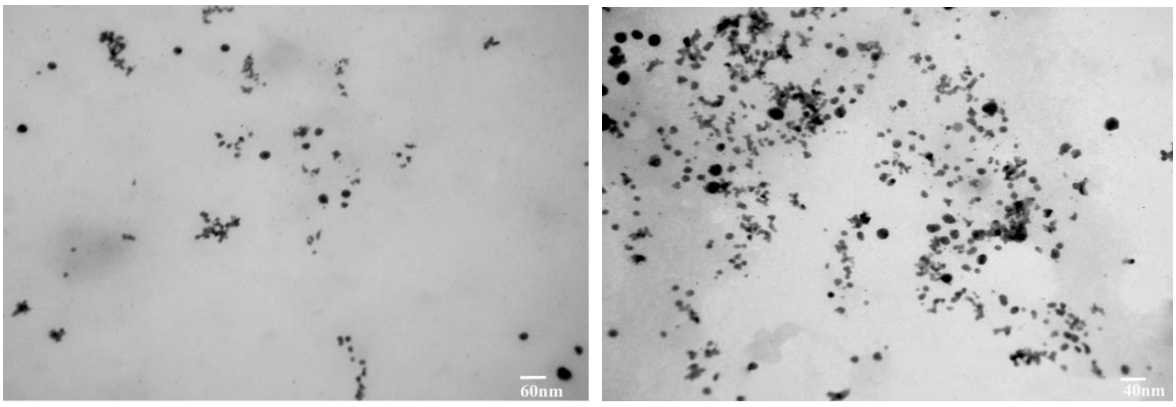

(**a**) (**b**)

Figure 8. (**a**) TEM Analysis of CSNp; (**b**) TEM Analysis of CNNp.

Energy dispersive X-ray spectroscopy

Energy dispersive X-ray spectroscopy (XRD) was used to determine the crystallographic structure of nanoparticles. XRD represents the crystalline nature of the gold nanoparticles that is prepared from CSE and CNW. The diffraction peaks of CSNp were observed at 38.17°, 44.66°, 66.13° and 76.19°, representing the intensity as (353.11), (141.1), (137.37) and (131.14). The diffraction peaks of CNNp were observed at 38.88°, 43.46°, 64.19° and 78.99°, representing the intensity as (255.13), (98.12), (92.11) and (105.22) which describe the crystalline structure of gold nanoparticles. XRD graphs were shown in Figure 9a,b.

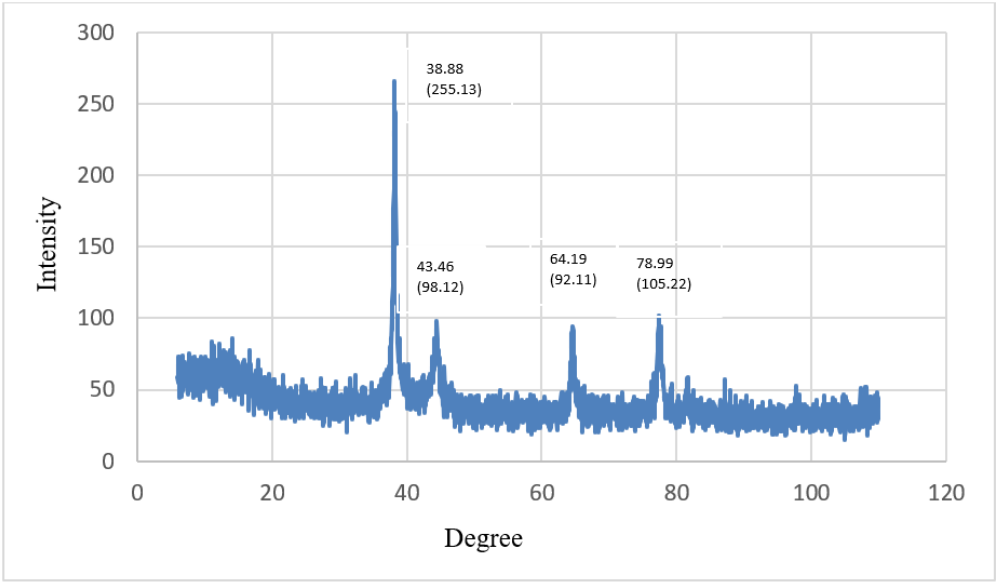

(**a**)

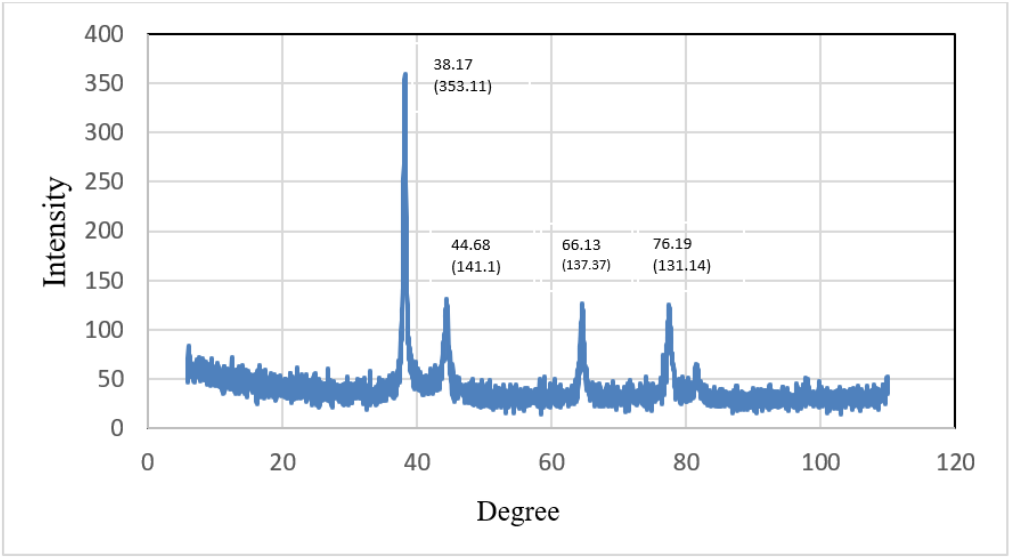

(**b**)

Figure 9. (**a**) X-ray diffractograms of CNNp; (**b**) X-ray diffractograms of CSNp.

UV-Visible spectroscopy

UV-Visible spectroscopy (UV-vis spectroscopy) was used to determine the absorbance of gold nanoparticles. The process of absorption and scattering of the light by gold nanoparticles, the color change of this reaction was consistent with occurrence of the maximum (λmax) of the localized surface plasmon resonance (LSPR) absorption band which occurs in the range of 520–570 nm. LSPR absorption band of green gold nanoparticles are shown in (Table 2). UV-Vis spectra of gold nanoparticles were shown in Figure 10a–c.

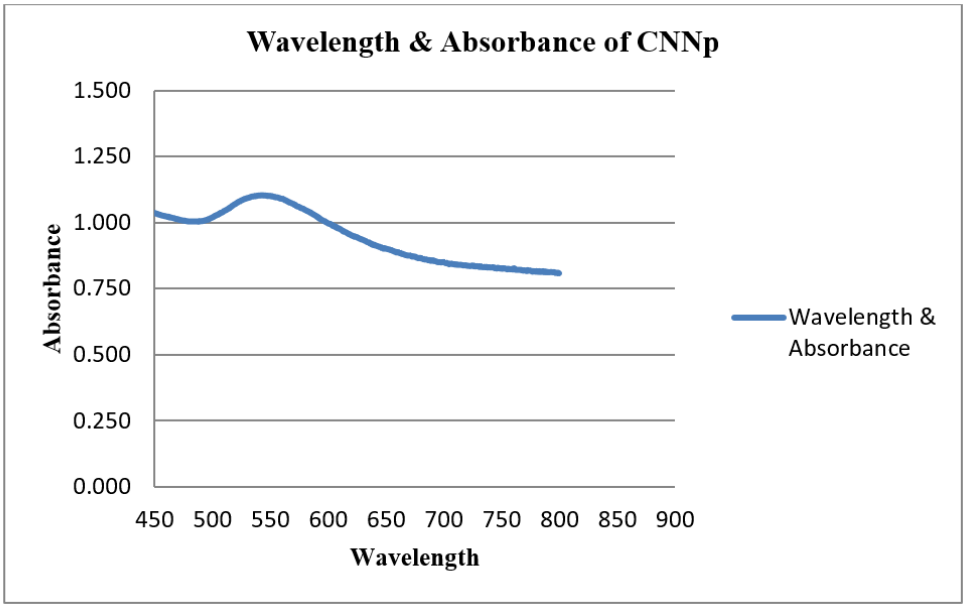

(**a**)

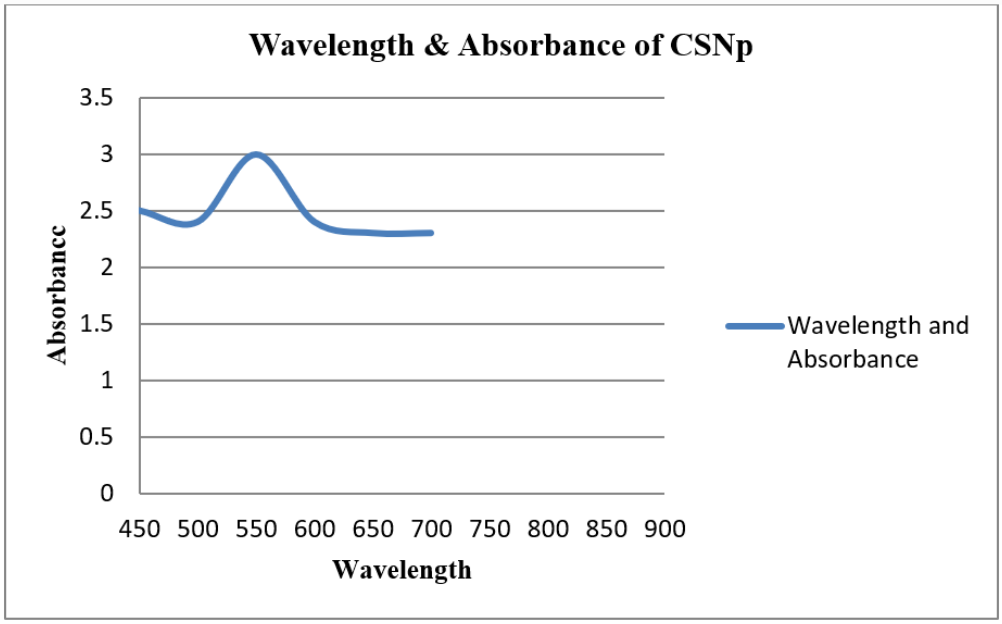

(**b**)

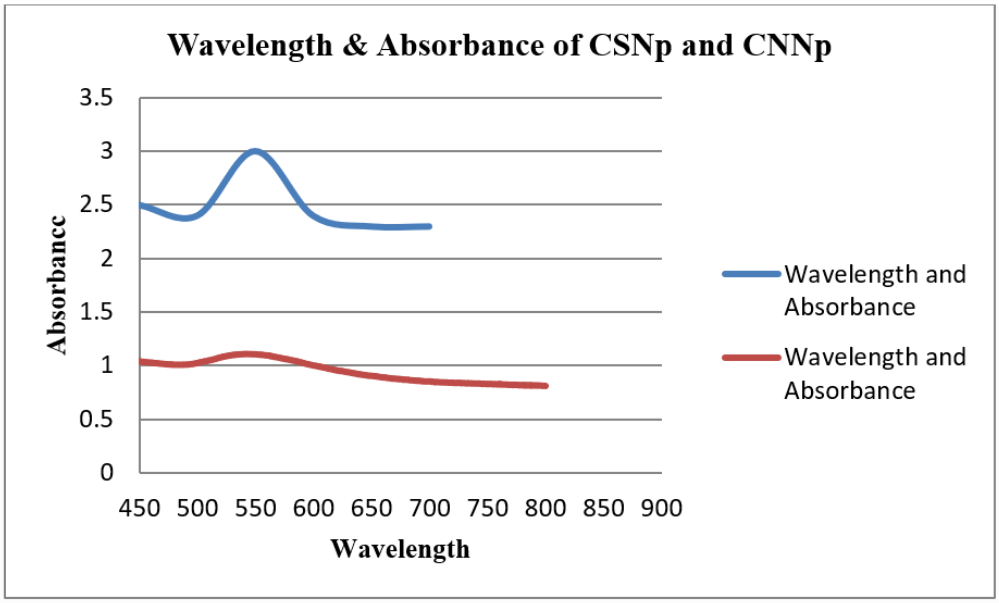

(**c**)

Figure 10. (**a**) UV-Vis spectra of CNNp; (**b**) UV-Vis spectra of CSNp; (**c**) UV-Vis spectra of CSNp and CNNp. Whereas Blue line and red line shows CSNp and CNNp respectively.

Table 2. Maximum value of localized surface plasmon resonance (LSPR) absorption band of prepared green gold nanoparticles.

Plants	Reducing agent	Concentration	λ_{max} (nm)
Camellia sinensis	*Camellia sinensis* leaves extract	3.9 mg/100µl	550
Cocos nucifera	*Cocos nucifera* water	3.9 mg/100µl	535

Antimicrobial activity:

Zone of inhibition

The zone of inhibition of CSE, CNW and gold nanoparticles was calculated against the pathogenic bacteria *Staphylococcus aureus*. Zone of inhibition were shown in Figure 11a,b.

(**a**) (**b**)

Figure 11. (**a**) Zone of inhibition of CSNp and CNNp against *Staphylococcus* aureus; (**b**) Zone of inhibition of CSE, CNW, CSNp and CNNp against *Staphylococcus aureus*. Whereas C: Green coconut (*Cocos nucifera*) gold nanoparticles; T: Green tea (*Camellia sinensis*) gold nanoparticles; Amp: Ampicillin (antibiotic); DW: Distilled water; GTE: Green tea (*Camellia sinensis*) extract; GTN: Green tea

(*Camellia sinensis*) gold nanoparticles; GCW: Green coconut (*Cocos nucifera*) water; GCN: Green coconut (*Cocos nucifera*) gold nanoparticles.

Zone of inhibition of CSNp is 13 mm; CNNp are 25 mm, ampicillin is 9 mm it considered there is no zone of inhibition in case of *Staphylococcus aureus*. Zone of inhibition of CSE is 10 mm and CSNp is 13 mm. zone of inhibition of CNW is 22 mm and CNNp is 25 mm. It means that gold nanoparticles have better results as compared to CSE and CNW.

Minimum inhibitory concentration (MIC)

MIC OF CSNp at 24 h incubation

The analysis of variance (Table 3) showed that the 24 h of incubation of *Staphylococcus aureus* with CSNp had significant effect on the OD value of culture and thus on the growth of *Staphylococcus aureus* ($p < 0.05$). Different concentrations of CSNp was performed MIC that are given in Tables 3 and 4.

Table 3. Analysis of variance for MIC of different concentrations of CSNp against *S. aureus* at 24 h incubation.

Analysis of Variance					
Source	**DF**	**Adj SS**	**Adj MS**	**F-Value**	***p*-Value**
Factor	3	725.9	241.96	7.42	0.011
Error	8	260.9	32.61		
Total	11	986.7			

* = Significant ($p < 0.05$).

Comparison of means showed significant difference among various test groups (Table 4). The lowest MIC was found in case of GTN1 (2.600 ± 1.126 ^{B} μg/mL) at 24 h of incubation. Comparison of means showed GTN to be significantly lower ($p < 0.05$) as compared to GTN3 and GTN4 while with GTN2, it showed non-significant difference ($p > 0.05$). On the other hand, the highest MIC was noted in case of GTN3 (20.00 ± 8.66 ^{A} μg/mL).

Table 4. Comparison of mean MIC of different concentrations of CSNp against *S. aureus.*

Different Concentrations of CSNp	**Mean ± SD**
GTN3 (30 mg/μL)	20.00 ± 8.66 ^{A}
GTN4 (50 mg/μL)	16.67 ± 7.22 ^{A}
GTN2 (10 mg/μL)	3.333 ± 1.444 ^{B}
GTN1 (3.9 mg/μL)	2.600 ± 1.126 ^{B}

Means that do not share a letter are significantly different.

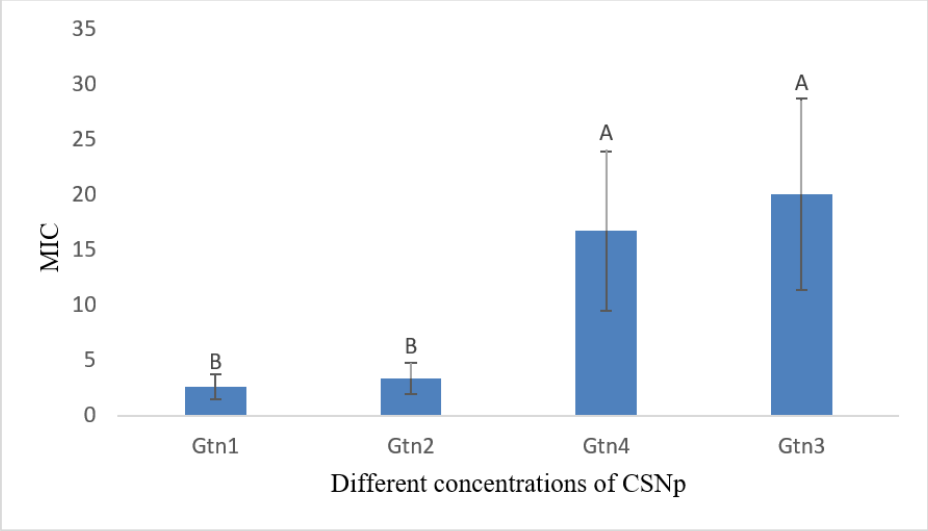

Figure 12. Graphical representation of mean MIC of different concentrations of CSNp against *S. aureus* at 24 h incubation.

MIC OF CNNp at 24 h incubation

The analysis of variance (Table 5) showed that the 24 h of incubation of *Staphylococcus aureus* with CNNp had significant effect on the OD value of culture and thus on the growth of *Staphylococcus aureus* ($p < 0.05$).

Table 5. Analysis of variance for MIC of different concentrations of CNNp against *S. aureus.*

Analysis of Variance					
Source	**DF**	**Adj SS**	**Adj MS**	**F-Value**	***p*-Value**
Factor	3	1826.7	608.89	8.08	0.008
Error	8	602.5	75.32		
Total	11	2429.2			

* = Significant ($p < 0.05$).

Comparison of means showed significant difference among various test groups (Table 6). The lowest MIC was found in case of GCN1 (3.250 ±1.126 ^{B} µg/mL) at 24 h of incubation. Comparison of means showed GCN1 to be significantly lower ($p < 0.05$) as compared to GCN4 while with all other preparations, it showed non-significant difference ($p > 0.05$). On the other hand, the highest MIC was noted in case of GCN4 (33.33 ±14.43 ^{A} µg/mL).

Table 6. Comparison of mean MIC of different concentrations of CNNp against *S. aureus* at 24 h of incubation.

Different concentrations of CNNp	**Mean ± SD**
GCN4 (50 mg/µL)	33.33 ±14.43 ^{A}
GCN3 (30 mg/µL)	19.17 ±9.46 ^{AB}
GCN2 (10 mg/µL)	4.167 ±1.443 ^{B}
GCN1 (3.9 mg/µL)	3.250 ±1.126 ^{B}

Means that do not share a letter are significantly different.

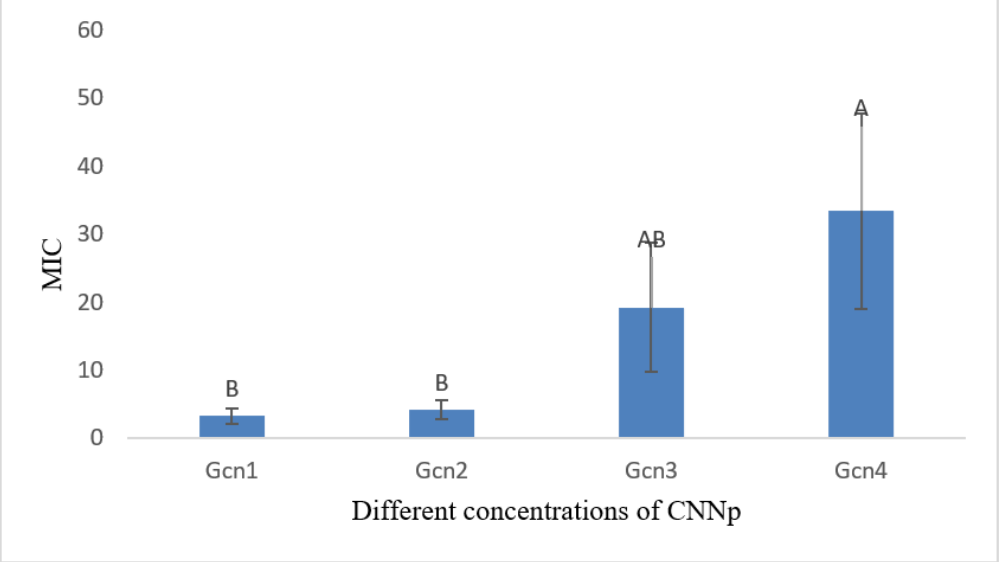

Figure 13. Graphical representation of mean MIC of different concentrations of CNNp against *S. aureus* at 24 h of incubation.

4. Discussion

Gold nanoparticles prepared by green plants do not require any external chemical agents for the reduction and stabilization of the nanoparticles. Phytochemical substances present in CNW or CSE are responsible for the formation of coating on gold nanoparticles and these nanoparticles were stable against agglomeration.

Nanoparticles have an extensive range of biological targets because of their smaller size so the zeta size and zeta potential are the most important features of nanoformulations [17]. Zeta potential was used to determine the surface charge of nanoparticles. Zeta size of CSNp and CNNp were 41.61 nm and 34.12 nm. Zeta potential of CSNp and CNNp were −16.52 mV and −14.61 mV. These results are align with the reference of [18,19].

UV-Visible spectroscopy was used to determine the absorbance of gold nanoparticles. The occurrence of the maximum (λmax) of the localized surface plasmon resonance (LSPR) absorption band, occur in the range of 520–570 nm for gold nanoparticles. The λmax of CSNp is 540 nm and CNNp is 524 nm. These conclusions are related with the quotation of [20].

Peaks of FTIR results give information that CSNp and CNNp both followed the same trends of peaks that confirm the preparation of green gold nanoparticles. These findings are similar with the reference of [21].

SEM gives information about the morphology of gold nanoparticles that is spherical shapes; these observations are in agreement to Yadav et al. who prepared nanoparticle using *Camellia sinensis.* CSNp shows no agglomerates. TEM gives the highly magnified images of gold nanoparticles that are prepared using CSE and CNW. These outcomes are alike with the allusion of [22].

The crystal structure of gold nanoparticles was presented by XRD. The diffraction peaks of green tea gold nanoparticles were observed at 38.17°, 44.66°, 66.13° and 76.19°, representing the intensity as (353.11), (141.1), (137.37) and (131.14). The diffraction peaks of green coconut gold nanoparticles were observed at 38.88°, 43.46°, 64.19° and 78.99°, representing the intensity as (255.13), (98.12), (92.11) and (105.22) which describe the crystalline structure of gold nanoparticles, these consequences are comparable with the mention of [23].

Antimicrobial action of green gold nanoparticles with a size range between 30–80 nm using the well diffusion method on an agar plate were determined and zone of inhibition of *S. aureus* was observed. The well diffusion method results of CSNp and CNNp against

S. aureus are shown in Figure 11a,b that are clearly show the zones of inhibition. Additionally, the zone of inhibition of CNNp is greater than the CSNp. These conclusions are similar with the discussion of [24]. MIC is the lowest concentration of antibacterial agents that inhibit the growth of bacteria by serial dilution. In Table 4, different concentrations of CSNp were showed the MIC value. GTN1 (3.9 mg/μL) show the lowest value of MIC that is (2.600 ± 1.126 ^{B}). In Table 6, different concentrations of CNNp were showed the MIC value. GCN1 (3.9 mg/μL) show the lowest value of MIC that is (3.250 ±1.126 ^{B}). These findings are similar with the reference of [25].

5. Conclusions

Gold nanoparticles of different size and shape were synthesized by CSE and CNW that act as a reducing and stabilizing agent without implicating different physical and chemical methods. Gold nanoparticles were prepared by biological method. This method is simple, eco-friendly, cost-effective and gives monodisperse, functional gold nanoparticles. Confirmation of gold nanoparticles was done by UV-Vis spectroscopy, DLS, FTIR, SEM, TEM and XRD. *Camellia sinensis* provided the formation of more stable nanoparticles and offered a wide range of particle sizes and shapes. In the current study, green gold nanoparticles showed excellent outcomes and maximum zones of inhibition against *S. aureus.* MIC was determined by Broth Micro Dilution method against *S. aureus.* MIC outcomes were in accordance with the zone of inhibition for example more zone of inhibition less MIC value and vice versa.

Abbreviations

CSE, *Camellia sinensis* extract; CNW, *Cocos nucifera* water; CSNp, *Camellia sinensis* gold nanoparticle; CNNp, *Cocos nucifera* gold nanoparticle; A, Ampicillin.

References

1. Steinig, E.J.; Duchene, S.; Robinson, D.A.; Monecke, S.; Yokoyama, M.; Laabei, M.; Slickers, P.; Andersson, P.; Williamson, D.; Kearns, A.; et al. Evolution and global transmission of a multidrug-resistant, community-associated methicillin-resistant staphylococcus aureus lineage from the Indian subcontinent. *MBio* **2019**, *10*, e01105-19. https://doi.org/10.1128/MBIO.01105-19.
2. O'Malley, S.M.; Emele, F.E.; Nwaokorie, F.O.; Idika, N.; Umeizudike, A.K.; Emeka-Nwabunnia, I.; Hanson, B.M.; Nair, R.; Wardyn, S.E.; Smith, T.C. Molecular typing of antibiotic-resistant Staphylococcus aureus in Nigeria. *J. Infect. Public Health* **2015**, *8*, 187–193. https://doi.org/10.1016/J.JIPH.2014.08.001.
3. Paharik, A.E.; Parlet, C.P.; Chung, N.; Todd, D.A.; Rodriguez, E.I.; Van Dyke, M.J.; Cech, N.B.; Horswill, A.R. Coagulase-Negative Staphylococcal Strain Prevents Staphylococcus aureus Colonization and Skin Infection by Blocking Quorum Sensing. *Cell Host Microbe* **2017**, *22*, 746-756.e5. https://doi.org/10.1016/J.CHOM.2017.11.001.
4. Aslam, B.; Arshad, M.I.; Aslam, M.A.; Muzammil, S.; Siddique, A.B.; Yasmeen, N.; Khurshid, M.; Rasool, M.; Ahmad, M.; Rasool, M.H.; et al. Bacteriophage Proteome: Insights and Potentials of an Alternate to Antibiotics. *Infect. Dis. Ther.* **2021**, *10*, 1171–1193. https://doi.org/10.1007/S40121-021-00446-2.
5. Aggarwal, S.; Jena, S.; Panda, S.; Sharma, S.; Dhawan, B.; Nath, G.; Singh, N.P.; Nayak, K.C.; Singh, D.V. Antibiotic Susceptibility, Virulence Pattern, and Typing of Staphylococcus aureus Strains Isolated From Variety of Infections in India. *Front. Microbiol.* **2019**, *10*, 2763. https://doi.org/10.3389/FMICB.2019.02763.
6. Gour, A.; Jain, N.K. Advances in green synthesis of nanoparticles. *Artif. Cells Nanomed. Biotechnol.* **2019**, *47*, 844–851. https://doi.org/10.1080/21691401.2019.1577878.
7. Akhtar, B.; Muhammad, F.; Aslam, B.; Saleemi, M.K.; Sharif, A. Pharmacokinetic profile of chitosan modified poly lactic co-glycolic acid biodegradable nanoparticles following oral delivery of gentamicin in rabbits. *Int. J. Biol. Macromol.* **2020**, *164*, 1493–1500. https://doi.org/10.1016/J.IJBIOMAC.2020.07.206.
8. Salem, S.S.; Fouda, A. Green Synthesis of Metallic Nanoparticles and Their Prospective Biotechnological Applications: An Overview. *Biol. Trace Elem. Res.* **2021**, *199*, 344–370. https://doi.org/10.1007/s12011-020-02138-3.
9. Muhammad, F.; Nguyen, T.D.T.; Raza, A.; Akhtar, B.; Aryal, S. A review on nanoparticle-based technologies for biodetoxification. *Drug Chem. Toxicol.* **2017**, *40*, 489–497. https://doi.org/10.1080/01480545.2016.1277736.
10. Geraldes, A.N.; da Silva, A.A.; Leal, J.; Estrada-Villegas, G.M.; Lincopan, N.; Katti, K.V.; Lug&atildeo, A.B. Green Nanotechnology from Plant Extracts: Synthesis and Characterization of Gold Nanoparticles. *Adv. Nanoparticles* **2016**, *05*, 176–185. https://doi.org/10.4236/anp.2016.53019.
11. Moongraksathum, B.; Chen, Y.W. Anatase TiO2 co-doped with silver and ceria for antibacterial application. *Catal. Today* **2018**, *310*, 68–74. https://doi.org/10.1016/j.cattod.2017.05.087.

12. Ganachari, S.V.; Yaradoddi, J.S.; Somappa, S.B.; Mogre, P.; Tapaskar, R.P.; Salimath, B.; Venkataraman, A.; Viswanath, V.J. Green nanotechnology for biomedical, food, and agricultural applications. In *Handbook of Ecomaterials*; Springer International Publishing:Berlin/Heidelberg, Germany, 2019; Volume 4, pp. 2681–2698, ISBN 9783319682556.
13. Katas, H.; Moden, N.Z.; Lim, C.S.; Celesistinus, T.; Chan, J.Y.; Ganasan, P.; Suleman Ismail Abdalla, S. Biosynthesis and Potential Applications of Silver and Gold Nanoparticles and Their Chitosan-Based Nanocomposites in Nanomedicine. *J. Nanotechnol.* **2018**, *2018*, 4290705. https://doi.org/10.1155/2018/4290705.
14. Manandhar, S.; Luitel, S.; Dahal, R.K. In Vitro Antimicrobial Activity of Some Medicinal Plants against Human Pathogenic Bacteria. *J. Trop. Med.* **2019**, *2019*, 1895340. https://doi.org/10.1155/2019/1895340.
15. Shamaila, S.; Zafar, N.; Riaz, S.; Sharif, R.; Nazir, J.; Naseem, S. Gold nanoparticles: An efficient antimicrobial agent against enteric bacterial human pathogen. *Nanomaterials* **2016**, *6*, 71. https://doi.org/10.3390/nano6040071.
16. Elbehiry, A.; Al-Dubaib, M.; Marzouk, E.; Moussa, I. Antibacterial effects and resistance induction of silver and gold nanoparticles against Staphylococcus aureus-induced mastitis and the potential toxicity in rats. *Microbiologyopen* **2019**, *8*, 698. https://doi.org/10.1002/MBO3.698.
17. Bhattacharjee, S. DLS and zeta potential—What they are and what they are not? *J. Control. Release* **2016**, *235*, 337–351. https://doi.org/10.1016/J.JCONREL.2016.06.017.
18. Yaqoob, S.B.; Adnan, R.; Rameez Khan, R.M.; Rashid, M. Gold, Silver, and Palladium Nanoparticles: A Chemical Tool for Biomedical Applications. *Front. Chem.* **2020**, *8*, 376. https://doi.org/10.3389/FCHEM.2020.00376.
19. Anwar, M.; Muhammad, F.; Aslam, B.; Saleemi, M.K. Isolation, characterization and in-vitro antigenicity studies of outer membrane proteins (OMPs) of Salmonella gallinarum coated gold nanoparticles (AuNPs). *Immunobiology* **2021**, *226*, 152131. https://doi.org/10.1016/J.IMBIO.2021.152131.
20. ElMitwalli, O.S.; Barakat, O.A.; Daoud, R.M.; Akhtar, S.; Henari, F.Z. Green synthesis of gold nanoparticles using cinnamon bark extract, characterization, and fluorescence activity in Au/eosin Y assemblies. *J. Nanoparticle Res.* **2020**, *22*, 309. https://doi.org/10.1007/S11051-020-04983-8.
21. Clarance, P.; Luvankar, B.; Sales, J.; Khusro, A.; Agastian, P.; Tack, J.C.; Al Khulaifi, M.M.; AL-Shwaiman, H.A.; Elgorban, A.M.; Syed, A.; et al. Green synthesis and characterization of gold nanoparticles using endophytic fungi Fusarium solani and its in-vitro anticancer and biomedical applications. *Saudi J. Biol. Sci.* **2020**, *27*, 706–712. https://doi.org/10.1016/J.SJBS.2019.12.026.
22. Rodríguez-León, E.; Rodríguez-Vázquez, B.E.; Martínez-Higuera, A.; Rodríguez-Beas, C.; Larios-Rodríguez, E.; Navarro, R.E.; López-Esparza, R.; Iñiguez-Palomares, R.A. Synthesis of Gold Nanoparticles Using Mimosa tenuiflora Extract, Assessments of Cytotoxicity, Cellular Uptake, and Catalysis. *Nanoscale Res. Lett.* **2019**, *14*, 334. https://doi.org/10.1186/S11671-019-3158-9.
23. Doan, V.D.; Huynh, B.A.; Nguyen, T.D.; Cao, X.T.; Nguyen, V.C.; Nguyen, T.L.H.; Nguyen, H.T.; Le, V.T. Biosynthesis of Silver and Gold Nanoparticles Using Aqueous Extract of Codonopsis pilosula Roots for Antibacterial and Catalytic Applications. *J. Nanomater.* **2020**, *2020*, 8492016. https://doi.org/10.1155/2020/8492016.
24. Folorunso, A.; Akintelu, S.; Oyebamiji, A.K.; Ajayi, S.; Abiola, B.; Abdusalam, I.; Morakinyo, A. Biosynthesis, characterization and antimicrobial activity of gold nanoparticles from leaf extracts of Annona muricata. *J. Nanostructure Chem.* **2019**, *9*, 111–117. https://doi.org/10.1007/S40097-019-0301-1.
25. Loo, Y.Y.; Rukayadi, Y.; Nor-Khaizura, M.A.R.; Kuan, C.H.; Chieng, B.W.; Nishibuchi, M.; Radu, S. In Vitro antimicrobial activity of green synthesized silver nanoparticles against selected Gram-negative foodborne pathogens. *Front. Microbiol.* **2018**, *9*, 1555. https://doi.org/10.3389/FMICB.2018.01555/BIBTEX.